sea state cci

Data Access Requirement Document (DARD)

version 1.1, 27 March 2019

Contents

1. Introduction 3

2. List of data and access requirements 4

2.1 Altimetry data 4

2.2 SAR data 4

2.3 In situ data 5

2.4 Microseism data 7

3. References 8

Author	Approved	Signature	Date
Ellis Ash	Fabrice Ardhuin		27/03/19

Issue	Date	Comments
0.5	14 Dec 2018	Full draft for internal review
1.0	5 Feb 2019	First version for review by ESA
1.1	27 Mar 2019	Table added for microseism data

Digitally signed by Craig Donlon
Date: 2019.03.27 14:13:42 Z
Adobe Acrobat DC version: 2015.006.30464

1. Introduction

This document presents the Data Access Requirement Document (DARD) for **Sea_State_cci**, deliverable 1.3 of the project. This first version is prepared early in the project in order to list the input data required and any access constraints and conditions. An updated version will be produced towards the end of the project.

The remainder of this Data Access Requirements Document contains a list of data and access requirements and / or a description of data, broken into subsections according to category as follows:

- Altimetry data
- SAR data
- in situ data
- Microseism data

In general the data required are publicly available, and there are no access constraints unless otherwise stated.

2. List of data and access requirements

2.1 Altimetry data

The list of the input altimetry product required for the CCI project is as follows:

Product	Source	Volume over CCI time frame, in TB	Temporal coverage	Access
S-GDR Jason-2	Aviso+ or NODC	currently: 3.1 TB	Jul 2008 - ongoing	open and public
S-GDR Jason-3	Aviso+ or NODC	currently: 0.4 TB	Feb 2016 - ongoing	open and public
RA2_MWS_2P EnviSat	ESA	2.9 TB	June 2002 - Apr 2012	open and public
S-GDR AltiKa	CNES/ Aviso+	currently: 3 TB	March 2013 - ongoing	open and public
Cryosat-2 L1B LRM L1B SIR L1B SI	ESA	currently: 1.5 TB 0.7 TB 5.3 TB	2010 - ongoing	open and public
S3A_SR_1_SRA_A_ Sentinel-3 L1A data (*)	EUMETSAT		2017-2018	open and public
S3A_SR_2_WAT Sentinel-3A + SR_1_SRA_BS___N TC SR_1_SRA_A_ (L1A)	Eumetsat	currently: 3.2 TB	Dec 2016 - ongoing	open and public
S3B_SR_2_WAT Sentinel-3B+ possibly some L1 (*)	Eumetsat		2018 - ongoing	open and public

Note: Jason-1, ERS-1 & 2, TOPEX/Poseidon, GFO and GeoSat altimeters are left out during the first project phase. An archive of these product's waveforms is however available already on Ifremer platform as they were used for Ifremer/CNES Altiberg project (http://cersat.ifremer.fr/about-us/projects/item/402-altiberg) .

2.2 SAR data

The SAR wave mode data currently hold at Ifremer cover the need of the project, they are summarized here:

Product	**Source**	**Volume over CCI time frame, in TB**	**Temporal coverage**	**Access**
ERS-1 wave mode L1	ESA/F-PAF (Ifremer)	9.5	1991-1996	restricted; available to project
ERS-2 wave mode L1		11.5	1995-2011	
Envisat/ASAR wave mode L1	ESA/F-PAF (Ifremer)	27.6	2003-2012	
Sentinel-1A wave mode L1	ESA	455	2014-2020	open and public
Sentinel-1B wave mode L1		309	2016-2020	

2.3 In situ data

Moored buoys with more than 10 years of data that are sufficiently far from coastlines in deep water are important reference time series for validation and calibration of the satellite observations. Buoys from the NDBC, CDIP, MEDS, and OCEANSITES networks with these criteria are shown in the following Figure 1. More importantly, these data will help in validating the consistency of the satellite records for climate applications.

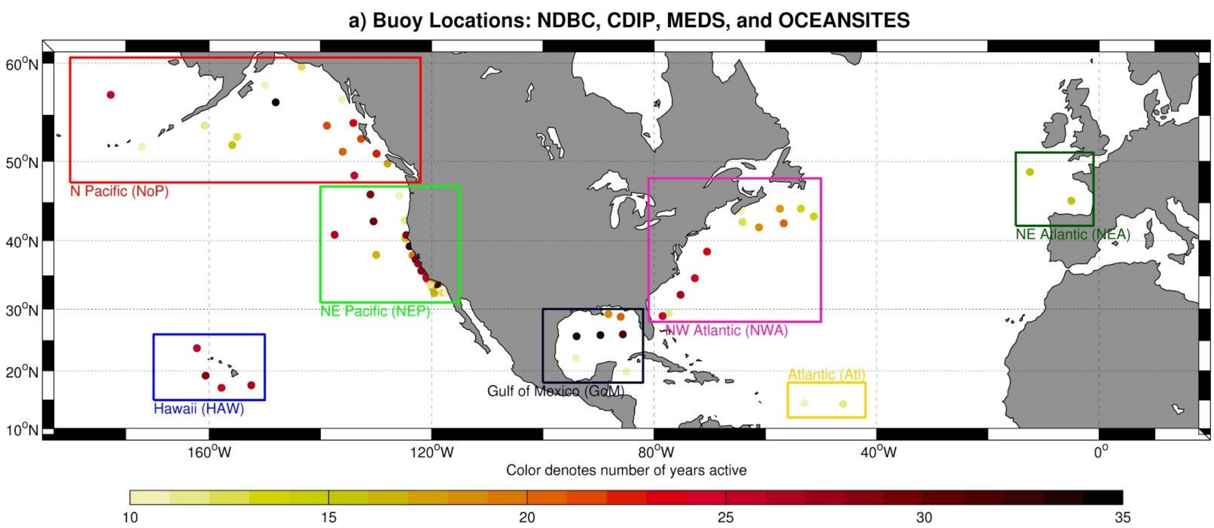

Figure 1: Buoys with at least 10 years of observations, >50 km from the coast, and in deep water. The color code represents the length of the buoy time series in years.

A major concern of the time series from the moored buoys is the consistency. Changes in sensor payloads, geographical displacements, sensor configurations (e.g. placement of the sensors on the buoy), and hull type all affect the homogeneity of the historical records. Changes due to these issues were observed on buoys from the MEDS and NDBC networks in the NE Pacific (Gemmrich et al., 2011). These calibration issues are more widespread and exist on buoys near Hawaii, Gulf of Mexico, and NW Atlantic (Livermont, 2017). It is proposed that a subset of the buoys, possibly those with the longest time series, shown in the above figure are analyzed in more detail assessing the consistency utilizing the metadata describing the payload and hull changes. For this endeavor we propose to use existing tools such as RHtestV4 developed to assess homogeneity in time series developed by Wang and Feng (2013). This task will be performed in collaboration with Bob Jensen of the USACE and Ian Young of University of Melbourne.

For the **in situ wind and wave** measurements that will be used for the validation of CCI products, the project will rely on the **CMEMS in situ TAC** that collects all buoy data from the following sources:

- NDBC (including CDIP)
- MEDS
- CEREMA
- Meteo-France
- various buoys over European seas over Baltic, Azores, Spain, Portugal, Greece

This service takes over the task previously performed through **ESA/GlobWave** project and both teams work together to ensure a smooth and seamless transition. By April 2018, it will provide the full backlog for all these networks, as well as the wave spectra when available, and will then be a major asset for the CCI Sea State project.

The data are full homogenized (variable names and format), quality controlled and delivered in NetCDF format. The illustration below shows the coverage over September 2017.

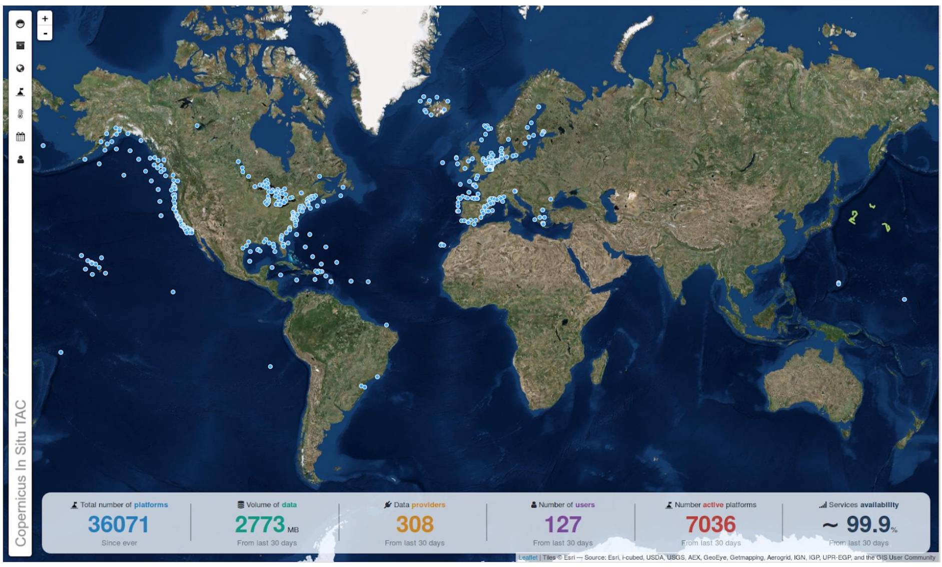

Figure 2: Coverage of in situ data over September 2017

2.4 Microseism data

Seismic records of ground displacement anywhere on Earth contain the signature of ocean waves in a broad frequency band that typically ranges from 0.003 Hz to 1 Hz, this signature is known as microseisms. The quantitative link between waves and microseism is well understood for the vertical displacements in the “secondary microseism” peak that is around 0.2 Hz (e.g. Bernard 1941, Longuet-Higgins 1950, Hasselmann 1963, Ardhuin & Herbers 2013). This is dominated by Rayleigh waves generated where ocean waves of opposing direction and same frequency are found in the ocean. Such seismic sources can be put in three broad classes of events (Ardhuin et al. 2011).

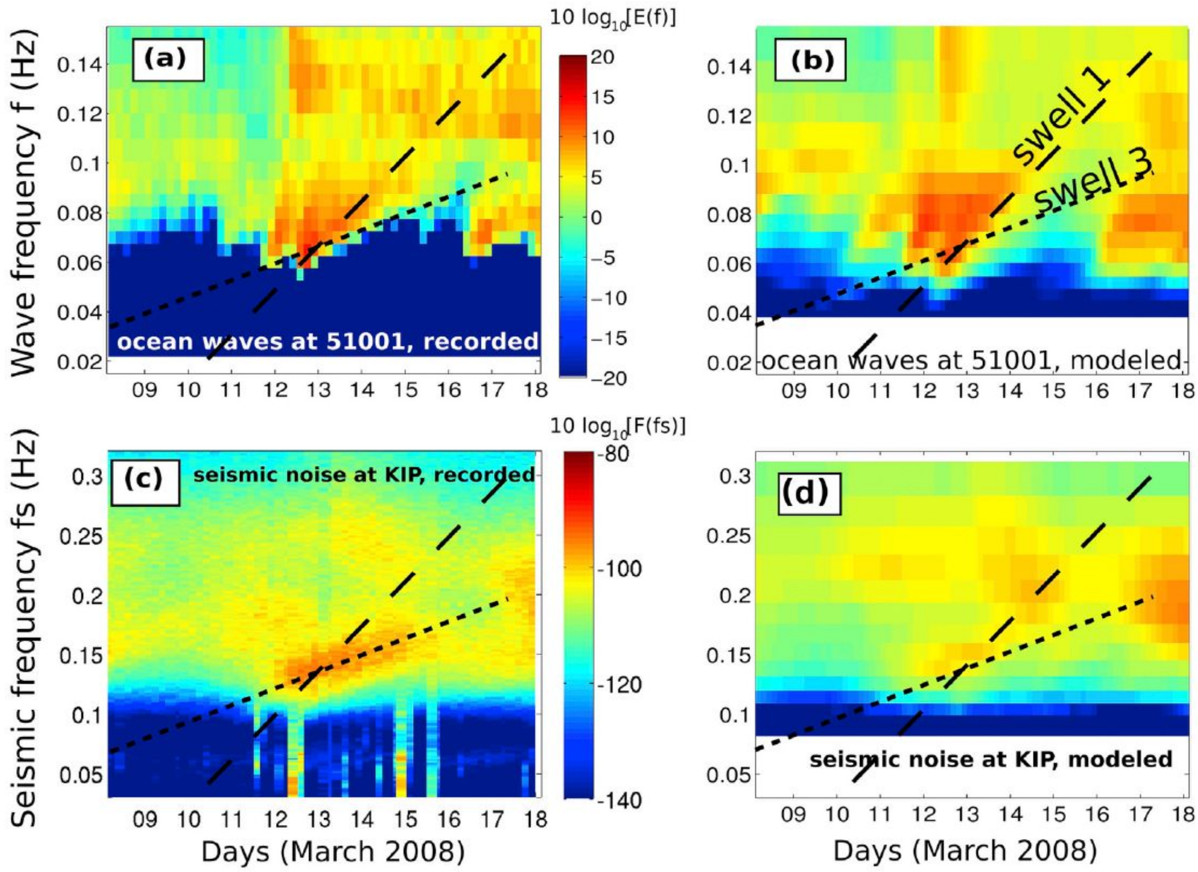

Figure 3: Example of seismic spectrogram (bottom) observed and modeled, compared to wave spectra (top). Taken from Ardhuin et al. (2011).

Due to the importance of opposing directions, there is no simple relation between wave height and microseism amplitude. However, for a same ocean wave spectrum shape, an increase in microseism correspond to an increase in wave height. As a result, microseism amplitudes can be use to track the magnitude of ocean waves over time (Bernard 1990, Grevemeyer et al. 2000). Any given station gives some sea state index in a region that varies in size from a few hundreds of kilometers to a few thousand of kilometers with a clear influence of regional sea ice for example (Stutzmann et al., 2009, Stutzmann et al. 2012, Sergeant et al. 2013). Furthermore, secondary microseism can provide independent constraints on the amount of ocean wave reflection coefficient.

The seismic data product and access is summarised here:

Product	**Source**	**Volume over CCI time frame**	**Temporal coverage**	**Access**
GEOSCOPE Seismic	IPGP	1TB	1982 - ongoing	Open access

data doi:10.18715/GEOSCOPE.G	Datacenter			by request to IPGP

The processed data will include all Geoscope stations (see map below, http://geoscope.ipgp.fr/index.php/en). Data are converted into seismic acceleration and spectrogram are computed using windows of 3 hours. Three-hourly spectra data for the vertical components with 512 frequencies takes about 7 Mb for a full year. The total volume for 40 stations over 30 years is only 8 Gb, including quality flags indicating the likely occurrence of earthquakes. Synthetic spectrograms will be computed and the comparison between observed and modelled spectrogram will enables to constrain the ocean wave coastal reflection coefficient.

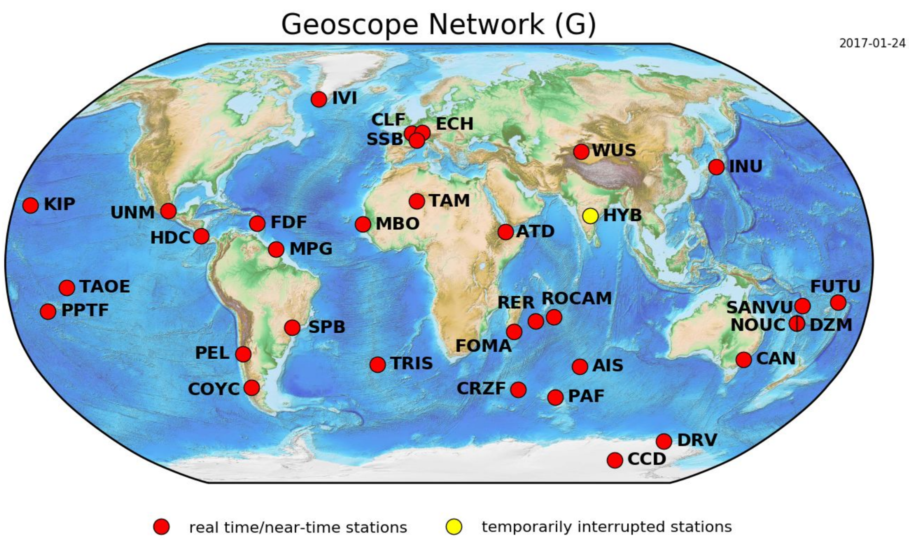

Figure 4: Extension of the Geoscope network of seismic stations

Ongoing developments on seismic array processing also shows that a single array can be used to get a map of microseism sources (Farra et al., 2015, Meschede et al., 2017). We will further explore the capability of using long-term arrays such as the Grafenberg array for mapping sources and their evolution over the past 40 years.

3. References

Ardhuin, F., Stutzmann, E., Schimmel, M., and Mangeney, A., "Ocean wave sources of seismic noise," J. Geophys. Res., 116, p. C09004, 2011. doi:10.1029/2011JC006952.

Ardhuin, F. and Herbers, T. H. C., "Noise generation in the solid earth, oceans and atmosphere, from nonlinear interacting surface gravity waves in finite depth," J. Fluid Mech., 716, 316–348, 2013. doi:10.1017/jfm.2012.548.

Bernard, P., "Sur certaines proprietes de la boule etudiées a l'aide des enregistrements seismographiques," Bull. Inst. Oceanogr. Monaco, 800, 1–19, 1941.

Bernard, P., "Historical sketch of microseisms from past to future," Phys. Earth Planetary Interiors, 63, 145–150, 1990. doi:0031-9201(90)90013-N.

Farra V., E. Stutzmann, L. Gualtieri, M. Schimmel and F. Ardhuin. Ray-theoretical modeling of secondary microseism P-waves. 2016, Geoph. J. Int., 206, 1730-1739, doi: 10.1093/gji/ggw242

Gemmrich, J., B. R. Thomas, and R. Bouchard, **2011**: Observational changes and trends in northeast Pacific wave records. Geophys. Res. Lett., 38, L22601, doi:10.1029/2011GL049518.

Grevemeyer, I., Herber, R., and Essen, H.-H., "Microseismological evidence for a changing wave climate in the northeast Atlantic Ocean," Nature, 408, 349–351, 2000.

Grob, M., Maggi, A., and Stutzmann, E., "Observations of the seasonality of the antarctic microseismic signal, and its association to sea ice variability," Geophys. Res. Lett., 38, p. L11302, 2011. doi:10.1029/2011GL047525.

Hasselmann, K., "A statistical analysis of the generation of microseisms," Rev. of Geophys., 1, 2, 177–210, 1963.

Livermont, E., 2017. Correcting changes in the NDBC wave records of the United States. 15th International Workshop on Wave Hindcasting and Forecasting, Liverpool, UK, September 10-15.

Longuet-Higgins, M. S., "A theory of the origin of microseisms," Phil. Trans. Roy. Soc. London A, 243, 1–35, 1950.

Meschede M., E. Stutzmann, V. Farra, M. Schimmel, F. Ardhuin. The effect of water column resonance on the spectra of secondary microseism P waves 2017 J. Geophys. Res., 122, 8121-8142., doi:10.1002/2017JB014014

E. Stutzmann, M. Schimmel, G. Patau, A. Maggi. Global climate imprint on seismic noise. 2009, Geochemistry, Geochem. Geophys. Geosyst., 10, Q11004, doi:10.1029/2009GC002619

Stutzmann E. , F. Ardhuin, M. Schimmel, A. Mangeney, G. Patau, Modelling long-term seismic noise in various environments 2012, Geoph. J. Int, doi:10.1111/j.1365-246X.2012.05638.x

Wang, X. L. and Y. Feng, published online July 2013: RHtestsV4 User Manual Climate Research Division, Atmospheric Science and Technology Directorate, Science and Technology Branch, Environment Canada. 28 pp. [Available online at http://etccdi.pacificclimate.org/software.shtml]